stellarator news

Published by Fusion Energy Division, Oak Ridge National Laboratory
Building 9201-2; P.O. Box 2009; Oak Ridge, TN 37831-8071, USA

Editor: James A. Rome Issue #16 July, 1991

8th International Workshop on Stellarators, Kharkov, USSR, May 27–31, 1991

This biennial workshop, an IAEA Technical Committee Meeting, is the major conference in the stellarator area. The three previous workshops were held in Oak Ridge (1989), Kyoto (1986), and Schloss Ringberg (1984); the next International Stellarator Workshop is proposed for Germany in 1993. There were 101 participants from 10 Soviet institutions and 25 participants from Germany, Japan, Spain, the United States, and the IAEA. The five-day workshop featured 10 overview talks on the major existing and planned stellarators and 95 other presentations on a wide range of topics: magnetic configurations, plasma production and heating, MHD equilibrium and stability, transport, fluctuations, the plasma edge, diagnostics, and future experiments.The conference proceedings will be distributed by the IAEA, and a summary of the workshop will be published in *Nuclear Fusion.*

Considerable progress has been made in stellarator research during the past year. The Heliotron-E group has concentrated on studies of core and edge transport, measurements of the divertor stripe, plasma current measurements, and development of high-power 106-GHz ECH. CHS experiments have focused on vertical field control during neutral beam heating, toroidal plasma rotation, magnetic field perturbation studies, and ICRF heating. Both groups are making progress in understanding the improvement in confinement that occurs with inward shifts of the magnetic axis. ATF has focused on long-pulse (< 20-s) operation, fluctuation studies, and the use of configuration variations for study of the dissipative trapped electron mode. W VII-AS has made significant improvements in performance with boronization of the vacuum vessel: $T_e(0) < 3$ keV, $T_i(0) < 0.45$ keV, $\nu^* = 10^{-3}$, $n_e < 5 \times 10^{19}$ m^{-3}, and $\tau_E < 35$–40 ms with 0.8-MW ECH and $T_e(0) = T_i(0) < 0.5$ keV, $\nu^* = 0.1$, $n_e < 3 \times 10^{20}$ m^{-3}, $\langle\beta\rangle < 0.7\%$, and $\tau_E < 25$–30 ms with 1.5-MW NBI; previously, NBI plasmas had been limited to $n_e < 8 \times 10^{19}$ m^{-3} and $T_e < 600$ eV by a radiative collapse due to metallic impurities. The rebuilt Uragan-3M has a larger plasma ($a_p = 12$ cm), and its energy confinement is 1.3–1.5 times that obtained in Uragan-3.

Good progress is also being made toward new experiments. In Spain, the TJ-I Upgrade torsatron ($R_0 =$ 0.6 m) should start operation by the end of the year, and the TJ-II flexible heliac ($R_0 = 1.5$ m) is under construction. In the USSR, the new Uragan-2M torsatron and upgrades to the L-2 stellarator should be completed by the end of the year. LHD ($R_0 = 3.9$ m, $a_p = 0.65$ m, $V_p =$ 30 m^3, $B_0 = 4$ T, $P > 20$ MW) appears to be on schedule for an April 1997 startup, and the W VII-X proposal (R_0 = 5.5 m, $a_p = 0.53$ m, $V_p = 30$ m^3, $B_0 = 3$ T, and P > 10 MW) is in the midst of a Phase I (programmatic) review by Euratom.

Stellarators are also being used to improve our understanding of tokamaks through basic studies of instabilities and transport that use the stellarator's ability to vary magnetic configuration properties in a controlled way that is not possible on a tokamak. The similarity of behavior and confinement for a wide range of stellarator and tokamak configurations and the insensitivity to imposed field errors on ATF and CHS and to resonances in W VII-AS at higher density suggest the universality of toroidal confinement behavior.

James F. Lyon
Oak Ridge National Laboratory
P.O. Box 2009, MS 8072
Oak Ridge, TN 37831-8072, USA

ATF coil accident

ATF had a flashover near a joint region on one helical field (HF) coil during a 2-T shot on May 30, 1991. An upper HF segment was removed for damage inspection and repair. There were three punctured internal water lines in the upper segment and one in the adjoining lower HF segment. There is no evidence yet as to the cause of the accident, but primary candidates remain a water leak and debris. The repairs have begun. The removed upper segment has been cleaned, and its insulation tests were successful. Cleanup of the damaged lower segment is now in progress. When the insulation test is completed, the repaired upper segment will be reinstalled. The goal is to run ATF to complete some unfinished experiments this fiscal year. Operation will be limited to 1-T, short pulse (< 2-s) operation because of reduced cooling of the segments. At least three turns in the damaged segments will not be water cooled because of leaks. Duty cycle, repetition rate, and shot limit per day will be determined by cooling limits.

Thomas C. Jernigan
Oak Ridge National Laboratory
P.O. Box 2009, Building 9201-2
Oak Ridge, TN 37831-8072, USA

Status of the Uragan-2M project

Construction of Uragan-2M — a torsatron with an additional toroidal field — is nearly complete at the Kharkov Institute of Physics and Technology. All elements of the last part of the machine, the $l = 2$, $m = 4$ helical winding, were manufactured by May. Now they are fixed in place on a supporting half-torus.

The rest of the device, namely the vacuum chamber, 16 toroidal field (TF) coils, and eight poloidal field (PF) coils, was assembled in February. The vacuum chamber was tested for leaks; some minor leaks were fixed. The TF and PF coils were used as a load for testing the new power supply system (250-MW ac flywheel generator with thyristor rectifiers) and all of the bus work.

Assembly of the device is scheduled to be complete at the end of September 1991. First measurements of flux surfaces for U-2M will start in October.

Our main efforts are now aimed toward fabrication of the rf antennas for the U-2M heating system. This system consists of three RF oscillators: RFO-1 and RFO-2 ($f = 10$–65 MHz, $P = 6$ MW, $t = 0.3$ s), and RFO-3 ($f = 325$ MHz, $P = 1.5$ MW, $t = 0.1$ s). Two helical antennas are designed for U-2M: (1) the slow wave antenna ($N_{\parallel} = 20$) with an area of 1 m^2 and $P = 3$ MW and (2) the fast wave antenna with an area of 2 m^2 and $P = 10$ MW.

The first antenna will be used for plasma production and preheating. The second one can be excited from two oscillators with different frequencies and will be used for electron and ion heating. First plasma experiments for U-2M will start at the end of this year.

Oleg Pavlichenko for the U-2M group
Institute of Physics & Technology
310108 Kharkov, USSR

Around the Labs

Status of CHS

Ion cyclotron heating experiments have been continued using two poloidal half-turn antennas located at two adjacent positions of the same helical pitch angle of the $m = 8$ CHS device. The main objective of the experiments during this experimental period, lasting until mid-August, is to find optimum conditions for heating efficiency both in the ion cyclotron resonance configuration (or rf frequency) and in the minority ion concentration. The results will be reflected in the arrangement of rf heating configuration and scenario in the next RF heating experimental plan in 1992, using more antennas with higher power.

As reported in the previous *Stellarator News*, we have succeeded in heating the plasma with only rf heating at a power level of 200 kW, although the increased radiation loss terminates hot plasmas [$T_e(0) = 100$–200 eV].

Experiments have been carried out with a mixed gas of hydrogen or helium-3 minority in deuterium gas by changing the ratio of the minority species and by changing the magnetic field strength (the location of the resonance layer). Two antennas are used, in phase or out of phase. The heating efficiency is apparently better with the out-of-phase configuration. A typical experimental scenario is shown in Figs. 1 and 2, together with the temporal evolution of the central electron temperature and density measured by Thomson scattering. The experimental conditions are as follows; $B = 0.9$ T, ECH (53 GHz) = 140 kW, ICH (14 MHz) = 200 kW out of phase. The ion cyclotron resonance layer is located

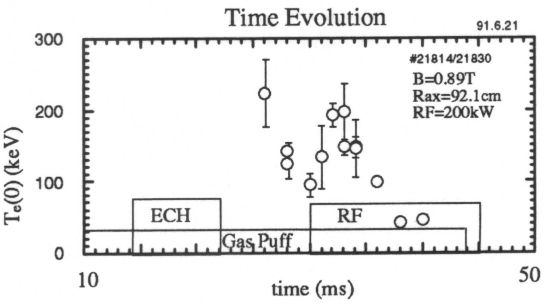

Fig. 1. Temperature in CHS during rf heating.

around one-third of the plasma radius at the low-field side. Although the hydrogen atom concentration is 2% using gas puffing, the number measured by visible spectroscopy is about 9%. This is considered to be due to hydrogen atoms released from the vacuum wall during the discharge.

Both electron and ion heating have been observed during the rf heating phase regardless of initially low electron temperatures. The electron density and temperature profiles in the rf heating phase are both parabolic, as opposed to the flattened density and peaked temperature profiles in the ECH phase. This is partially because the ion cyclotron resonance layer is located at an off-axis position and partially because the power deposition profile is believed to be broad. It is also observed that the edge density profile shrinks in the rf heating phase compared with the ECH phase.

Experiments were also carried out with helium-3 minority at the same frequency ($B = 1.4$ T). The electron temperature increased up to 350 eV and the ion temperature up to 300 eV (measured with a fast neutral analyzer) at the average density of 1.5×10^{13} cm^{-3}. In this operation, radiation loss decreased and the hot plasma lasted longer. Two possible reasons for this result are the increased magnetic field strength and the longer heating phase due to the reduced radiation loss.

Harukazu Iguchi for CHS Group
National Institute for Fusion Science
Nagoya 464-01, Japan

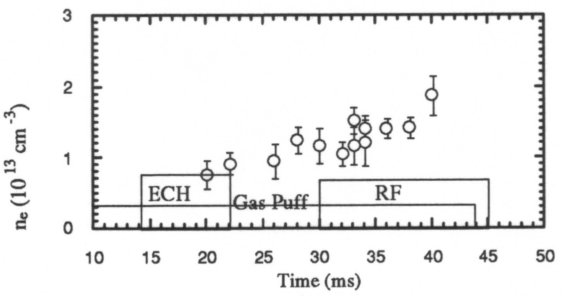

Fig. 2. Density in CHS during rf heating.

First experiments with 140-GHz ECRH at W7-AS

Pilot 140-GHz ECRH experiments with the second harmonic extraordinary mode were performed for the first time on the W7-AS stellarator. The gyrotron used is a prototype in the development line of the Kernforschungszentrum Karlsruhe (KfK) with a capability of 0.1-MW microwave power for 0.1-s pulse duration in the TE_{03} mode with 98% mode purity.

The microwaves are transmitted from the gyrotron to the W7-AS torus over a distance of about 30 m by an optical system. It consists of a set of imaging mirrors, a polarizer system for arbitrary choice of the wave polarization, and a new device for in situ power monitoring. This transmission line was developed by the Institut für Plasmaforschung, Stuttgart (IPF), and is designed for future 1-MW microwave power transmission.

The most promising aspect of 140-GHz ECRH is the extension of the accessible density to twice the value of the existing 70-GHz system, i.e. the cutoff density is 1.2×10^{20} m^{-3} at the resonant magnetic field of 2.5 T. This will open a new parameter window, once sufficient power is available. The electron-ion coupling is expected to be strong under these high-density conditions with the consequence of increased ion temperatures during ECRH. This is in contrast to the 70-GHz experiments, where the ions in general remain energetically decoupled from the electrons.

The high-density operation also offers the opportunity to combine powerful NBI and ECRH, which is not possible with the 70-GHz ECRH because of the particle fuelling by NBI and the correlated density increase beyond cutoff.

With this general motivation, the experiments performed so far have been aimed at demonstrating the high-density application of ECRH, while maintaining a narrow and well-localized power deposition profile. Due to the limited available source power of 100 kW, the investigations were performed as perturbation experiments, where about 65 kW of ECRH power was added to an NBI-sustained discharge. A pulse train consisting of a 70-GHz pulse and a successive 140-GHz pulse, each with 0.1-s pulse width, was launched into an NBI-heated target plasma, where the density was ramped from 0.4 to 1.4×10^{20} m^{-3}. The pulse train was shifted in time from low to high density. At densities below the 70-GHz cutoff, central electron heating was measured by ECE for both pulses. For the higher densities of up to 1.2×10^{20} m^{-3}, an increase of the central electron temperature was observed only during 140-GHz ECRH.

Finally, at a density above 1.2 $\times 10^{20}$ m^{-3}, this heating effect also vanished, as expected from the 140-GHz cutoff at 2.5 T.

A second experiment was dedicated to heat wave propagation by a modulation of the 140-GHz power. Both the power deposition profile and the electron heat diffusivity can be derived from the measurement of the phase shift and amplitude decay of an electron temperature modulation generated by a 100% amplitude modulation of the incident microwave beam. This method was applied for the first time to an NBI-heated target plasma with a constant density well above the 70-GHz cutoff. Preliminary results from the heat wave propagation analysis indicate a well-localized power deposition region and allow a direct determination of the electron heat diffusivity. In the modulated mode, the 140-GHz pulse can be extended to 0.5-s duration.

Supported by these encouraging results, we plan to install a more powerful 140-GHz gyrotron as soon as it is available. For a later stage of the experiments in W7-AS, a complete replacement of the existing 70-GHz installation by a 2-MW 140-GHz system is foreseen.

Volker Erckmann
for the W7-AS Team, IPP,
and the ECH Teams at KfK and IPF
Max-Planck Institut für Plasmaphysik
W-8046 Garching bei München, Germany

Reduced Shafranov shift in W7-AS from X-ray profile analysis

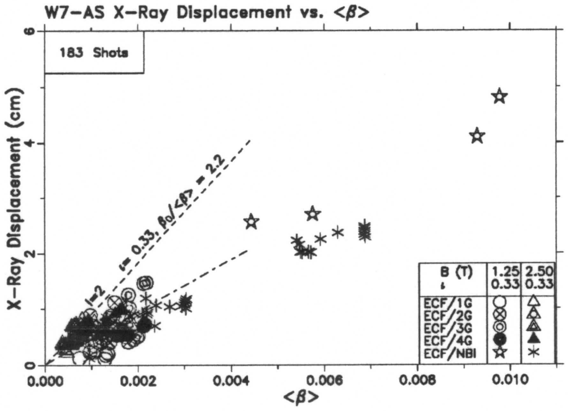

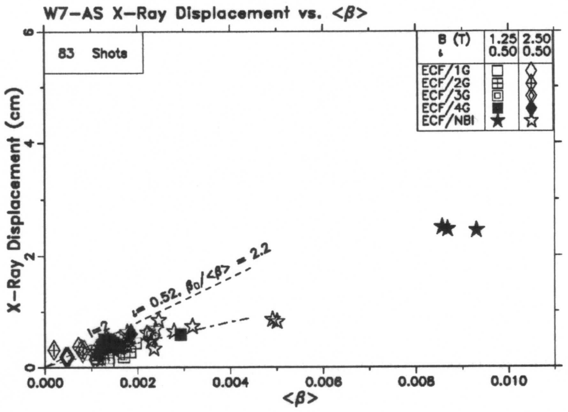

The Shafranov shift as a function of ⟨β⟩ in W7-AS for different experimental conditions.

In the last experimental campaign on W7-AS, considerable progress has been achieved in extending the operational range by carbonization and boronization of the vacuum vessel, resulting in reduced radiation losses. In ECRH discharges the density could be increased up to the cutoff value of 6×10^{19} m^{-3}, even with an ECRH power below 200 kW. In NBI discharges, at absorbed power values up to 1.5 MW, the radiative density limit could be raised to about 3×10^{20} m^{-3} as the peak value of a rather broad density profile at 2.5 T.

High-beta studies became possible at 1.25 T, half the maximun magnetic field. Although the confinement in the low magnetic field case was lower than that with the full field, maximum volume-averaged beta values of about 1.1% could be reached. The corresponding value at 2.5 T was 0.7%, correlated with a plasma energy inreasing slowly from 30 to 34 kJ within about 150 ms. This energy increase is caused by an increase of the line-averaged density from 1.5 to 1.8×10^{20} m^{-2}; peak values of the Thomson scattering profiles were 2.5 $\times 10^{20}$ m^{-3} for the electron density, and 0.32 keV for the electron temperature. The rotational transform was ι = 0.35 for this discharge.[1] The ion temperature should be close to that of the electrons.

In W7-AS, the Pfirsch-Schlüter currents are reduced by a factor of about two, as compared to those of a classical $l = 2$ stellarator. Therefore, the plasma position still changes significantly with respect to the vacuum configuration for beta values in the percent range. An important issue in W7-AS is to demonstrate the reduction of the Pfirsch-Schlüter currents experimentally as a proof of the optimization principle of the Advanced Stellarator concept. This is done by comparing the experimentally observed Shafranov shift in W7-AS with calculated values for the magnetic field configuration of W7-AS and a classical stellarator.

The horizontal plasma displacement was determined from the X-ray profiles in an energy range above 2 keV, observed by a camera system with 12 radial channels.

The first moments of the line-integrated intensity distributions are numerically analyzed and yield the Shafranov shift of the plasma center. The data given in the figures refer to different experimental conditions in W7-AS at particular times where Thomson scattering profiles have been measured, as a function of the volume-averaged beta. For certain discharges the X-ray displacement derived from the moments method was checked with tomographic reconstructions of the local X-ray emissivity. Good agreement was seen.

The result of the statistical analysis is separated for the cases of $\iota = 1/3$ and $\iota = 1/2$ in the two figures. The observed displacements are higher at low rotational transform, reaching values of about 5 cm, to be compared with an average plasma radius of 18 cm. For such extreme cases, time-dependent vertical fields were applied. For intermediate cases, preset vertical fields with some inward start position were used, and low-beta cases did not require an additional vertical field. The experimental data are in accordance with the values predicted for W7-AS on the basis of the Kisslinger-Wobig equilibrium code[2] shown as dot-dash lines. The predictions for a classical $l = 2$ stellarator are higher by a factor of about 2, as indicated by the dashed lines.

In the next experimental campaign on W7-AS, further improvements of the performance are expected from the modification of in-vessel components, i.e., replacement of TiC-coated graphite tiles on the two limiters by bulk boronized graphite, removal of the experimental ICRH antenna and its guard limiters, and improved shielding of magnetic pickup coils.

1. A. Weller et al., W7-AS Team, NBI Team, ICRH Group, PSI Group, Invited paper at 18th EPS Conf., Berlin 1991.

2. J. Kisslinger, H. Wobig, Proc. 12th EPS Conf., Budapest 1985, I, 453.

Arthur Weller for the W7-AS Team
Max Planck Institut für Plasmaphysik
W-8046, Garching bei München, Germany

Experiments on ATF

Operating experience during neutral beam injection (NBI) on ATF has shown that the available operating space (in terms of plasma electron density) is limited. Quasi-steady-state plasmas have only been attained in either extremely low-density (well below the ECH cutoff density, $n_e \leq 7.5 \times 10^{12}$ cm^{-3}) or extremely high-density ($n_e \geq 8.0 \times 10^{13}$ cm^{-3}) plasmas. For intermediate densities, the plasma either undergoes a thermal collapse (loss of all thermal energy) or has peculiar transient behavior. Three mechanisms have been proposed to explain the collapse: (1) impurity radiation, (2) excitation of an electron instability driven by the highly anisotropic nature of the NBI process, and (3) poor coupling of the beam ions to the background plasma. Detailed spectroscopic studies of plasma cleanliness have shown that radiation is an unlikely candidate for initiating these collapses, though it may become an important loss mechanism once the electron temperature has fallen to a low level. Also, a specific electron instability has not yet been identified during injection. However, recent experimental and computational work has shown that this limitation may be due to an unfavorable power balance at these intermediate densities.

The main diagnostic in these studies has been a two-dimensional scanning neutral particle analyzer (NPA). Using the scanning capability of the NPA, a rather complete measurement of the fast-ion distribution has been made during these intermediate-density discharges. Figure 1 shows a typical tangential spectrum measured at a time near the beginning of the thermal collapse in an intermediate-density discharge. The sharp decrease in the measured flux at energies below the three energy components of the beam is an indication that the con-

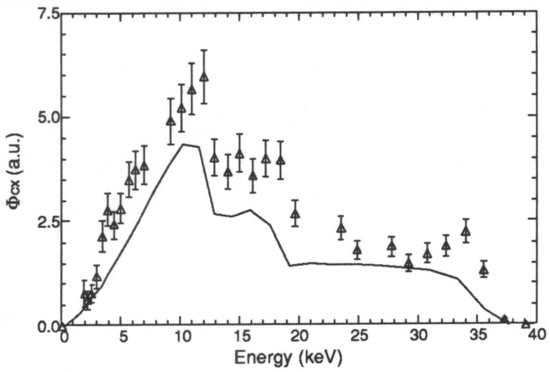

Fig. 1. Measured and simulated energy spectra for a tangential-viewing angle of the neutral particle analyzer on ATF.

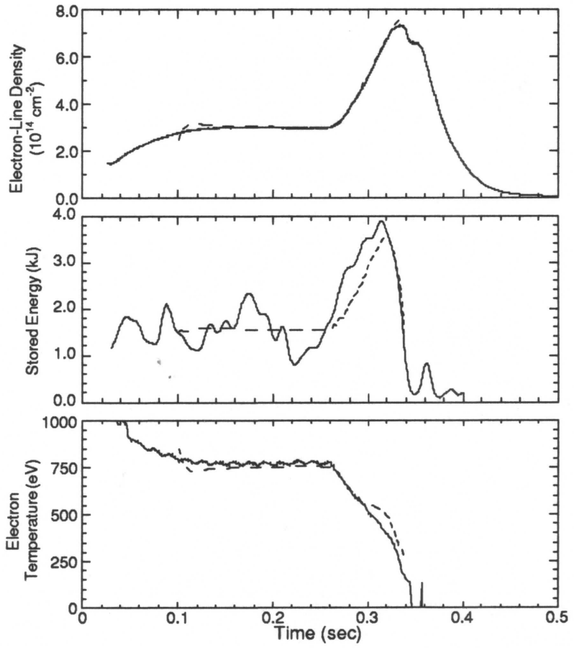

Fig. 2. Comparison between experimental data (solid lines) and PROCTR simulation (dashed lines) for a low-density NBI discharge in ATF. Approximately 600 kW of neutral beam power is injected at 250 msec for 100 msec.

finement of the injected ions is rather poor. Simulations of these measurements using a Fokker-Planck analysis code (shown as the solid line in Fig. 1) confirm these expectations and indicate that approximately 60% of the beam input power is not absorbed by the plasma (lost through either shinethrough or charge-exchange processes) at the time of the collapse. Further calculations using the Monte Carlo DESORBS code to simulate NBI in ATF confirm these large losses and also indicate that very little of the beam power is lost through orbit losses. This is theorized to be due to the fact that the fast-ion slowing-down time in this case is much longer than the charge-exchange time, so the tangentially injected ions do not experience much pitch-angle scattering before being lost because of charge-exchange.

To determine whether this reduced coupling is the cause of the thermal collapse, the PROCTR transport analysis code has been used to model the plasma evolution during these discharges. The agreement between the simulation and the measured data is quite good, as shown in Fig. 2. This simulation is quite sensitive to the ECH absorbed power near the time of the collapse and the impurity radiation after the collapse. In the simulation, the plasma does not undergo a thermal collapse unless the ECH absorbed power drops to zero near the time of the collapse. Furthermore, the complete collapse is strictly dependent on a large increase in the impurity radiation after the collapse. The unstable nature of the collapse is due to the unstable dependence of the impurity line radiation on the plasma electron temperature. For temperatures below 100 eV, any decrease in temperature results in an increase in the line radiation, which further cools the plasma. The electron temperature profile typically collapses inward from the edge as large amounts of radiation from the outer region of the plasma progressively cool adjacent plasma until all the stored energy is radiated in a brief (5 to 10 msec) burst of radiation.

Mickey R. Wade for the ATF Team
ORNL and Georgia Institute of Technology
P.O. Box 2009, MS 8072
Oak Ridge, TN 37831-8072, USA

106-GHz ECH System for Heliotron-E

Recently, a 106-GHz, 0.5-MW gyrotron was installed in Heliotron-E. The main purpose is to study the heating efficiency of the second harmonic X-mode resonance and to produce a high-density ($n \approx 7 \times 10^{13}$ cm^{-3}) target plasma for NBI. The system consists of a 0.5-MW gyrotron with a $TE_{12,2}$ whispering gallery mode output, an optimized down-taper,[1] an improved efficiency quasi-optical mode converter, and an HE_{11} transmission line as shown in the figure.

The output power of the gyrotron can be varied from 100 to 500 kW by varying the beam current and anode voltage. The operation map (anode voltage vs main field strength) is ~1.5 to 2 times wider than the existing 200-kW pulse tube. The output mode is measured by a wave number spectrometer. Dominant $TE_{12,2}$ and other spurious TM modes are identified.

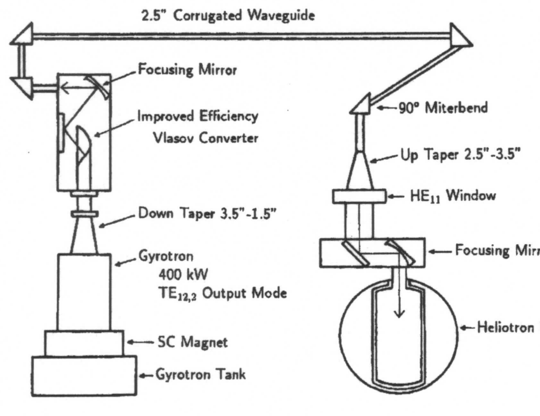

Fig.1 106GHz waveguide system for Heliotron-E

To convert the output whispering gallery mode to the HE_{11} linearly polarized Gaussian-like mode, a quasi-optical modified Vlasov antenna was developed.[2] The width of the phase correcting mirror, the axial length, and the helical cutting angle of the launcher are chosen to couple to the TEM_{00} mode. This new launcher was designed using geometrical optics so that the microwaves are radiated into a single mode determined by the plane wave expansion of whispering gallery modes. The visor and phase correcting mirrors are placed so that the rays do not hit the edge of the launcher. Cold tests showed that 93% of the microwave energy could be radiated to the Gaussian-like main lobe.

The HE_{11} transmission line consists of 18 m of tubular oversized waveguide (i.d. = 635 mm), four quasi-optical miter bends, up-taper (63.5 mm → 88.9 mm), vacuum-tight window, and focus mirror. The rectangular corrugation profile of the waveguide is as follows: mechanical slot depth $d_m = \lambda/4$ (λ = 2.82 mm), slot width w = 0.56 mm , and width/pitch w/p = 0.5. The vacuum-tight window is inserted between the waveguide and the Heliotron-E chamber.

The radiation patterns of the HE_{11} beam are measured by a set of microwave-absorbing screens and an infrared camera. The radiation pattern measured at the end of the waveguide showed that the solitary mode is HE_{11} within the resolution limit of the thermal image method. Extrapolating from beam diameters measured at different distances, we estimate that the e-folding beam diameter is approximately 30 mm at the end of the waveguide. This value assures good coupling efficiency to the 2.5-in. waveguide.

One of the 90° miter bends is used as a mode analyzer and bidirectional coupler by replacing the plane mirror with a multi-hole plate. The thickness of the plate, the diameter of the holes, and the spacing of the holes are 0.5 mm, 0.7 mm, and 2 mm, respectively. These parameters are chosen to get about −50 dB coupling. The signal from the holes is detected by a crystal diode mounted in a dominant-mode rectangular waveguide. The polarization can then be measured by rotating the waveguide. Since the results are similar to those measured by the thermal image method, this mode analyzer seems to be useful in monitoring the power profile. The polarization of the HE_{11} beam can be also obtained by the mode analyzer. The cross-polarization of the HE_{11} beam is high and is not changed after the 90° miter bend. Without the miter bend, the wave polarity was measured as a reference. It was compared with that obtained by the linear array, and they were in good agreement. Therefore, the mode analyzer gives the correct polarity of the high-power beam injected into plasmas.

Preliminary injection experiments were carried out using low power and a short pulse. The HE_{11} Gaussian-like beam is injected from the top side of the torus and absorbed at the second harmonic resonance. After the plasma was produced by 53-GHz fundamental harmonic heating, the 106-GHz power was injected for 17 ms. The plasma could be maintained only by 106-GHz second harmonic heating [$\bar{n} \approx (0.5{\sim}1.2) \times 10^{13}$ cm^{-3}]. The transmitted power, which is measured by a water load, is less than 200 kW, since the transmission line is not yet optimized. The electron temperature measured by Thomson scattering is approximately 800 eV, and the decay time of the ECE signal in the afterglow phase is about 12 ms.

With optimization of the transmission line, more power will be injected, and a higher density ($\leq 7 \times 10^{13}$ cm^{-3}) plasma will be heated. The 106-GHz heating experiment will restart this autumn.

1. M. Thumm, private communication.

2. M. Iima et al., 14th Int. Conf. Infrared and Millimeter Waves (Würzburg, 1989).

H. Zushi and K. Nagasaki for the Heliotron-E Group
Plasma Physics Laboratory
Kyoto University
Gokasho, Uji 611, Japan

People

Visiting Scientists

National Institute for Fusion Science

Dr. K. McCormick from the Max Planck Institut für Plasmaphysik at Garching, Germany, stayed at NIFS as a visiting professor for four months beginning in mid-February. He gave us useful suggestions for the improvement of a lithium neutral beam probe on CHS, based on his wide experience in ASDEX experiments.

Dr. M. Ueda from LAP/INPE at Sao Paulo, Brazil has been at NIFS on a one-year assingment since mid-March. He is working with the CHS group and is mainly engaged in a fast lithium neutral beam probe for edge diagnostics, especially near the separatrix area, which will be operational soon as a single-channel system.

Oak Ridge National Laboratory

Mikhail Shats and Konstantin Likin of the General Physics Institute (GPI), Moscow, arrived in late May for a three-month assignment. After the ATF coil repair, they will measure plasma turbulence in ATF using a 2-mm scattering diagnostic that was designed and constructed by the GPI. The microwave equipment was installed and checked out in early June, but the measurements will have to be delayed until the repair is completed.